Journal of Environmental Management 401 (2026) 128829

Contents lists available at ScienceDirect

Journal of Environmental Management

journal homepage: www.elsevier.com/locate/jenvman

Research article

Exploring the effects of carbon sources and exogenous electron donors on chain elongation in anaerobic mixed cultures

Merve Atasoy [a,b,c,d,*], Nicholas Stucki [a,b], Anna Jonkers [a,c], David Strik [a,b], Hauke Smidt [a,c]

[a] UNLOCK, Wageningen University & Research and Technical University Delft, Wageningen and Delft, the Netherlands
[b] Environmental Technology, Wageningen University & Research, PO box 8129, 6700 EV, Wageningen, the Netherlands
[c] Laboratory of Microbiology, Wageningen University & Research, the Netherlands
[d] Department of Chemistry and Sustainable Technology, University of Eastern Finland, Joensuu, Finland

ARTICLE INFO

Keywords:
Carboxylic acids
Medium chain fatty acids
Chain elongation
Mixed culture fermentation
Microbial community

ABSTRACT

The carboxylate platform offers a sustainable bioconversion strategy for biorefineries, utilizing anaerobic mixed cultures to produce carboxylate mixtures, including medium-chain fatty acids (MCFAs), as valuable intermediates. The effects of carbon sources (glucose, glycerol, casein) and exogenous supplied electron donors (ethanol, methanol, propanol, pyruvate) on MCFA production via chain elongation were investigated to elucidate the role of external electron donors and assess the feasibility of self-sufficient MCFA production in their absence. For this purpose, all experimental sets included corresponding control conditions without external electron donor addition. Batch experiments were conducted without active pH control, allowing pH to evolve dynamically in response to substrate type and metabolic activity. Results showed that the carbon source significantly affected carboxylic acid production and composition. Glucose primarily yielded propionate, independent of the electron donor. Casein resulted in the lowest carboxylic acid and gas production but uniquely produced the highest MCFA. Acidic pH conditions (5.0–5.5), which developed primarily in glucose- and glycerol-fed systems, favoured short-chain fatty acid production, whereas near-neutral pH conditions (6.0–6.7), observed in casein-fed systems, enhanced MCFA formation. Electron donors significantly influenced the degradation rate of glycerol. Methane production was observed in glucose and glycerol sets but was absent in casein sets. Microbial community analysis revealed methanogen dominance across most sets, irrespective of substrate. These findings highlight the complex interactions between pH, electron donor/acceptor availability, and microbial community dynamics in anaerobic digestion. Future multi-omics and flux analyses are needed to elucidate the metabolic pathways governing chain elongation and anaerobic digestion.

1. Introduction

The carboxylate platform presents a promising bioconversion strategy for sustainable biorefinery development, utilizing open mixed microbial cultures to generate carboxylate mixtures as intermediates for advanced biofuels and bioproducts (Agler et al., 2011; Holtzapple et al., 2022; Marzban et al., 2025). Carboxylates, organic acids with at least one carboxyl functional group, are primary fermentation products in anaerobic digestion. Short-chain fatty acids (SCFAs), intermediates of anaerobic digestion, are particularly valuable within this platform. These organic acids, typically containing 2–6 carbon atoms and commonly referred to as volatile fatty acids (VFAs), such as acetic, propionic, and butyric acids, serve as crucial industrial feedstocks and carbon sources for upstream bioprocesses (Atasoy et al., 2018). Despite their biobased potential, industrial SCFA production relies predominantly on petrochemical synthesis.

Major bottlenecks in transitioning to large-scale SCFA production arise from the need for sustainable and cost-effective separation and purification, complicated by their high solubility and volatility (Reyhanitash et al., 2016; Zacharof and Lovitt, 2014). On the other hand, SCFA can be elongated into medium-chain fatty acids (MCFAs, e.g., hexanoic, heptanoic, octanoic acids), which possess higher hydrophobicity, easing their separation and purification from effluent. Chain elongation processes can occur endogenously–where both the electron

* Corresponding author. Department of Chemistry and Sustainable Technology, University of Eastern Finland, Joensuu, Finland.
E-mail address: merve.atasoy@uef.fi (M. Atasoy).

https://doi.org/10.1016/j.jenvman.2026.128829
Received 10 July 2025; Received in revised form 9 January 2026; Accepted 31 January 2026
Available online 6 February 2026

donor and acceptor are generated through microbial conversion (with the donor formation referred to as endogenous electron donor formation)–or can be enhanced by supplying exogenous electron donors, such as ethanol, lactate, or reducing equivalents from electrodes, including H_2 and formate (Chatzipanagiotou et al., 2021; Jin et al., 2025; X. Li et al., 2024).

This conversion expands the application range and increases the economic value of the final products (Montecchio et al., 2024; Shrestha et al., 2022; Stamatopoulou et al., 2020; Undiandeye et al., 2024; Wang and Yin, 2022). Chain elongation (CE), a biochemical transformation carried by anaerobic microbial communities, converts SCFA to MCFA as a part of the anaerobic digestion pathway. Anaerobic digestion in open mixed cultures involves a complex cascade of biochemical reactions, where operational and environmental parameters can steer metabolic pathways towards CE or methanogenesis. Consequently, the resulting metabolite profiles are highly dependent on system conditions and microbial community composition (Spirito et al., 2014; Stamatopoulou et al., 2020; Wang and Yin, 2022).

The objective of this study is to investigate the influence of diverse model carbon sources (glucose, glycerol, and casein) on endogenous MCFA production in anaerobic mixed culture fermentation and the reveal effects on supply of ethanol, methanol, propanol and pyruvate. A seed material, anaerobic granular sludge from a paper-mill wastewater digester was used to explore its microbial potential. With this study, we hypothesize that manipulating these novel combinations of carbon source and electron donor availability can effectively control product spectrum due to the inherent flexibility of mixed cultures.

To further contextualize our research approach, we describe the role of the selected substrates. In the anaerobic digestion pathway (Fig. 1), complex organic compounds are initially hydrolyzed into simpler substrates. In this study, glucose, glycerol, and casein were used to represent carbon sources derived from carbohydrates, lipids, and proteins, respectively. Glucose, a readily degradable simple carbohydrate commonly used as a model substrate in anaerobic digestion studies, is metabolized to pyruvate via glycolysis (Hoelzle et al., 2014). Glycerol, although not a lipid itself, is a hydrolysis product of triglycerides and serves as a readily available lipid-derived substrate that can function as both a carbon and electron donor in chain elongation and other anaerobic pathways (Hoelzle et al., 2014; Leng et al., 2019; Stamatopoulou et al., 2020; Veras et al., 2020; Wang and Yin, 2022). Conversely, casein, a protein, undergoes anaerobic proteolysis, yielding amino acids (Bevilacqua et al., 2022; Deng et al., 2023). Subsequently, during acidogenesis, pyruvate and acetyl-CoA are fermented by primary fermenters, generating SCFA. This is followed by acetogenesis, where SCFA and other metabolites are converted to acetate, carbon dioxide, and hydrogen gas. While acidogenesis and acetogenesis appear straightforward, they encompass multiple biochemical reactions and diverse byproducts. These steps also involve β-oxidation of fatty acids and conversion of α-keto acids to organic acids (Spirito et al., 2014; Wang and Yin, 2022).

The metabolic pathway can then diverge towards either methanogenesis, producing methane and carbon dioxide, or chain elongation, leading to medium- and long-chain fatty acids. This branching is influenced by factors such as electron donor availability, pH, active microbial

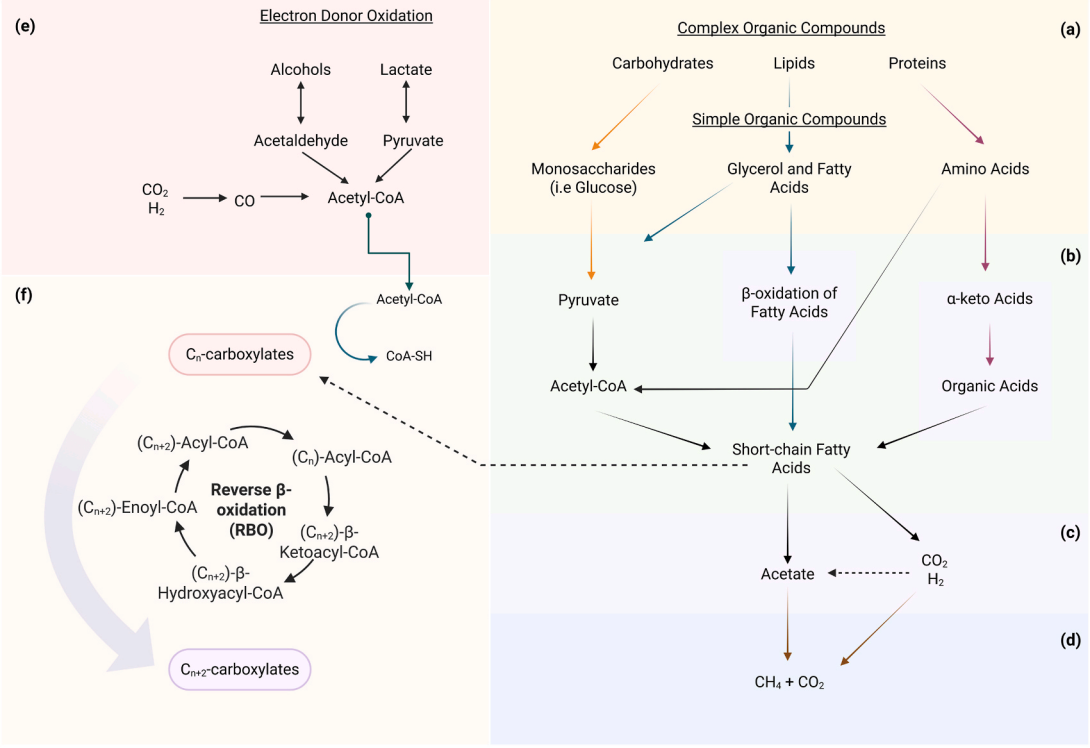

Fig. 1. Simplified anaerobic digestion metabolic pathway, illustrating the alternative routes between methanogenesis and chain elongation (CE) following post acidogenesis and acetogenesis. (a) During hydrolysis, complex organic matter is broken down into smaller molecules and fermented into short-chain carboxylic acids via acidogenesis (b). In acetogenesis (c), short-chain fatty acids are further converted into acetate and gaseous byproducts, including carbon dioxide and hydrogen. The β-oxidation of fatty acids and the conversion of α-keto acids into organic acids primarily lead to acetate formation, occurring in both acetogenesis and acidogenesis; hence, these processes are represented within phases (b) and (c). Following these stages, the metabolic pathway diverges. (d) Under neutral pH and low electron donor availability, methanogenesis dominates, resulting in methane production. In contrast, CE is favoured under slightly acidic conditions with an abundant supply of electron donors (e.g., ethanol, lactate) and controlled hydrogen partial pressure. Selective inhibition of methanogens further promotes CE. Electron donors are oxidized to Acetyl-CoA (e), which is subsequently incorporated into chain elongation pathways. The chain elongation pathway is illustrated (f) with the reverse β-oxidation (RBO) pathway. Adapted from Spirito et al. (2014), Dahiya et al. (2023), Wu et al. (2018), Wang et al. (2022) and Sikora et al. (2018). Created in https://BioRender.com.

groups and their functionalities, hydrogen partial pressure (Shrestha et al., 2023), and inhibitory side products like ammonia (Guo et al., 2023; Singh et al., 2023), hydrogen sulphide, and even salt concentration (Guo et al., 2023). If chain elongation is favoured, primarily reverse β-oxidation (RBO) is employed, depending on environmental conditions and microbial community composition (Leng et al., 2019). This pathway facilitates two-carbon extensions of starter molecules through cyclical biochemical reactions, with acetyl-CoA from electron donor oxidation playing a central role (Angenent et al., 2016; Spirito et al., 2014). RBO is widely recognized as the primary and most energy-efficient pathway for anaerobic carboxylic acid chain elongation (Scarborough et al., 2018). An overview of these anaerobic digestion metabolic pathways, including the positioning of chain elongation, is illustrated in Fig. 1.

As illustrated in Fig. 1, the CE pathways require external electron donors (e.g., alcohols) and acceptors (primarily SCFAs). Electron donors, defined as reduced compounds supplying energy, reducing equivalents (NADH), and acetyl-CoA, include a range of substrates, including alcohols, lactate, polysaccharides, and H_2/CO_2 (Han et al., 2018), which are converted to acetyl-CoA before entering the RBO pathway (Wang and Yin, 2022). MCFA yields have been shown to vary with electron donor, typically following the trend: ethanol > propanol > methanol (Spirito et al., 2014; Stamatopoulou et al., 2020; Wang and Yin, 2022).

Although traditional chain elongation relies on external electron donors, often from non-renewable sources, recent studies have demonstrated in-situ electron donor production from waste streams (Wang and Yin, 2022), including casein (Bevilacqua et al., 2022). This eliminates external donor requirements, promoting sustainability. However, anaerobic digestion is a complex process, susceptible to competing pathways, which can reduce chain elongation efficiency (Guo et al., 2023). Notably, chain elongation competes with methanogenesis, a syntrophic interaction involving methanogens (e.g., *Methanobacterium sp.*) and other bacteria (e.g., *Syntrophomonas sp.*), emphasizing the necessity for controlled conditions to favour MCFA production (Duber et al., 2024; Guo et al., 2023).

In the CE metabolic pathway, pH and electron donor/acceptor ratios are critical operational parameters. A pH of 5.0 was maintained to inhibit methanogenesis and maximize undissociated MCFA concentrations (pKa ~4.8), as neutral pH can favour methanogenesis (Candry et al., 2020; Coma et al., 2016; Fernández-Blanco et al., 2023, 2024) Optimal electron donor/acceptor ratios for MCFA production typically range from 2:1 to 4:1 (Angenent et al., 2016; Spirito et al., 2014; Stamatopoulou et al., 2020). An initial carbon source to electron donor ratio of 4:1 was used, adjusting to an effective ratio of 2:1 to account for in-situ electron acceptor generation. This study aims to identify how operational parameters influence the metabolic pathways in anaerobic digestion, specifically SCFA production, MCFA elongation, and methane formation, across different substrates as well as microbial community dynamics.

2. Materials and methods

2.1. Substrate and inoculum

This study investigated the influence of different carbon sources (carbohydrates, proteins, and lipids) and electron donors (EDs) on the chain elongation process. Glucose, glycerol, and casein were used as representative carbon sources derived from carbohydrates, lipids, and proteins, respectively. Glycerol was chosen as a readily available lipid-derived substrate that can serve as both a carbon and electron donor in chain elongation pathways. Ethanol, methanol, propanol, and pyruvate served as EDs, alongside a control set without added ED. Sodium pyruvate was used as pyruvate source. Each experimental set had a total soluble chemical oxygen demand (sCOD) of 8000 mg COD/L. For sets with added ED, the substrate concentration was 6000 mg COD/L, and the ED concentration was 2000 mg COD/L. The control sets contained 8000 mg COD/L of the respective substrate.

Anaerobic granular sludge, obtained from the anaerobic digester of a paper mill wastewater treatment plant (Eerbeek, the Netherlands) was used as inoculum. The sludge was stored at 4 °C for two weeks prior to use. The total solids (TS) and volatile solids (VS) content of the inoculum were 13 ± 0.75 % and 6.62 ± 1.7 %, respectively. A portion of the inoculum (10 g) was stored at −78 °C for microbial community analysis. The substrate-to-inoculum ratio, based on food-to-microorganism (F/M) ratio, was 1:2. The VS content of the inoculum was used for the M value, and the substrate sCOD was used for the F value.

The growth medium, based on OECD 311 guidelines, consisted of: 0.54 g/L KH_2PO_4, 2.24 g/L $Na_2HPO_4{\cdot}12H_2O$, 0.106 g/L NH_4Cl, 0.15 g/L $CaCl_2{\cdot}2H_2O$, 0.20 g/L $MgCl_2{\cdot}6H_2O$, 0.04 g/L $FeCl_2{\cdot}4H_2O$, and 0.004 g/L rezasurin (OECD, 2006). A trace element solution (10 mL/L) was added, containing: 2 mg/L $FeCl_2{\cdot}4H_2O$, 2 mg/L $CoCl_2{\cdot}6H_2O$, 0.32 mg/L $MnCl_2$, 0.024 mg/L $CuCl_2$, 0.05 mg/L $ZnCl_2$, 0.05 mg/L H_3BO_3, 0.09 mg/L $(NH_4)_6Mo_7O_{24}{\cdot}4H_2O$, 0.068 mg/L Na_2SeO_3, 0.05 mg/L $NiCl_2{\cdot}6H_2O$, 1 mg/L EDTA, and 0.001 mL/L HCl (36%). The vitamin solution, adapted from Atasoy et al. (2019), consisted of: 0.04 mg/L 4-aminobenzoic acid, 0.01 mg/L D(+)-biotin, 0.1 mg/L nicotinic acid, 0.05 mg/L calcium D (+)-pantothenate, 0.15 mg/L pyridoxine dihydrochloride, 0.1 mg/L thiamine, and 0.05 mg/L B_{12}.

2.2. Experimental design

Anaerobic batch experiments were conducted in 150 mL serum bottles (90 mL working volume) in biological triplicate. Reproducibility was confirmed by comparing trends across biological triplicates, and mean values with standard deviations are reported to show variation between replicates. The working volume comprised 15 mL of inoculum and 75 mL of growth medium with added substrates and/or EDs. The experiments were performed at 35 °C and pH 5, with continuous mixing at 120 rpm. The headspace of each bottle was flushed with nitrogen gas to establish anaerobic conditions. Samples were collected at retention times (RTs) of 1, 5, and 10 days.

2.3. Analytical methods

The performance of chain elongation was evaluated by monitoring sCOD, tCOD, gas composition, pH, conductivity, and concentrations of substrates, electron donors and metabolites. Prior to the experiments, sCOD and tCOD of the substrates and inoculum were measured. At each RT, gas samples were collected using a gas-tight syringe, and bottle pressure was measured using a Greisinger GMH 3151 pressure meter. After opening the bottles, pH and conductivity were measured. Supernatant samples were obtained by centrifugation (10,000 rpm, 4 °C, 3 min) and filtered (0.45 μm) for sCOD analysis. Total COD (tCOD) was measured on the un-filtered samples. COD was determined using Hach-Lange kits and a DR3900 spectrophotometer.

Gas composition (CH_4, CO_2, N_2) was analyzed using a Shimadzu GC-2010 gas chromatograph equipped with Porabond Q (50 m × 0.53 mm × 10 μm) and Molsieve 5A (25 m × 0.53 mm × 50 μm) columns. The oven and detector temperatures were 80 °C and 150 °C, respectively. Hydrogen (H_2) was measured using an HP 6890 gas chromatograph with an HP Molsieve 5A column (30 m × 0.53 mm × 25 μm) and a μ-TCD detector at 180 °C. The oven temperature was 40 °C.

Glucose and glycerol were quantified using a Thermo Dionex Ultimate 3000 RS high-performance liquid chromatograph (HPLC) with an OA-1000 organic acids column (300 mm × 6.5 mm) and a refractive index detector. The column temperature was 60 °C, and the eluent was 1.25 mM sulfuric acid at a flow rate of 0.6 mL/min.

Alcohols and carboxylic acids were analyzed using an Agilent 7890B gas chromatograph with an HP-FFAP column (25 m × 0.320 mm × 0.50 μm) and a flame ionization detector (FID) at 240 °C. Centrifuged supernatant samples were prepared with 15% formic acid. The oven temperature program was: 60 °C for 3 min, ramped to 140 °C at 21 °C/

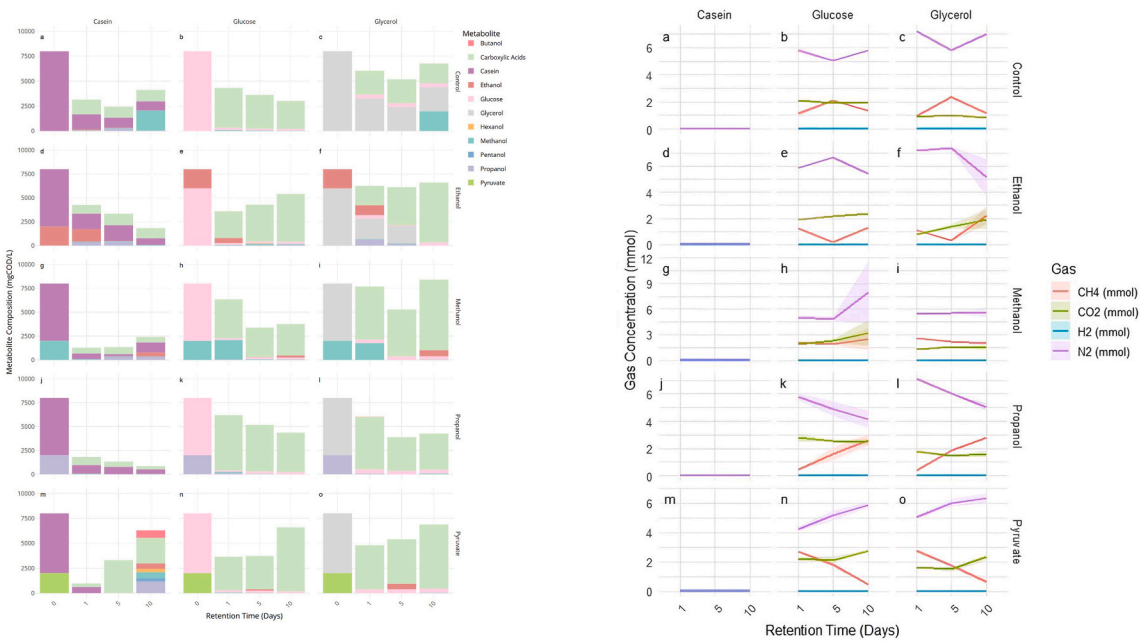

Fig. 2. (1) Temporal profiles of metabolite concentrations (mgCODeq/L) and (2) gas compositions (mmol) at 0, 1, 5, and 10 days of incubation for each carbon source (casein, glucose, glycerol) and electron donor (control, ethanol, methanol, propanol, pyruvate). The interactive plot displays the mean values of metabolites with corresponding standard deviations for each retention time point. It was generated using the Plotly. js library (v2.11.1).

min, to 150 °C at 8 °C/min (held for 1.5 min), to 200 °C at 120 °C/min (held for 1.25 min), and to 240 °C at 120 °C/min (held for 3 min). Nitrogen was used as the carrier gas. Samples for microbial community analysis (5 g) were stored at −78 °C.

2.4. Microbial community analysis

Microbial community composition was determined by Illumina sequencing of the 16S rRNA gene, following the protocol described by Atasoy et al. (2018). Total DNA was extracted from samples using the DNeasy PowerSoil Kit (QIAGEN, Germany) according to the manufacturer's instructions. DNA concentrations were quantified using a Qubit fluorometer (Thermo Fisher Scientific). 16S rRNA gene fragments were amplified using the 515F (5′-GTG CCA GCM GCC GCG GTAA) and 806R (5′-GGA CTA CHV GGG TWT CTA AT) primer pair (Caporaso et al., 2011; Klindworth et al., 2013). Sample-specific barcodes were added to the 5′ end of each primer. The PCR mixture (50 μL) contained 10 μL 5 × HF Green buffer (Thermo Fisher Scientific, the Netherlands), 1 μL Phusion Hot Start II High-Fidelity DNA polymerase (2 U, Thermo Fisher Scientific), 500 nM of each primer, 500 nM dNTPs (Promega, USA), 10 ng DNA template, and nuclease-free water (Promega, USA). The PCR program consisted of an initial denaturation at 98 °C for 30 s, followed by 25 cycles of denaturation at 98 °C for 10 s, annealing at 50 °C for 10 s, and elongation at 72 °C for 10 s, with a final extension at 72 °C for 7 min. PCR products were pooled and purified using CleanPCR beads (cleanNA, the Netherlands) according to the manufacturer's protocol. The purified amplicons were pooled in equimolar concentrations, along with a negative control (nuclease-free water). The 16S rRNA gene amplicon library was sequenced on an Illumina NovaSeq platform (Novogene, UK, Cambridge) generating 250 bp paired-end reads. Raw sequence data have been deposited in the NCBI Sequence Read Archive (SRA) under BioProject accession number PRJEB89878.

2.5. Bioinformatics and statistical analysis

Raw sequencing data were processed using the computational workflow described by Koehorst and Nijsse (2021) (Koehorst and B. Nijsse, 2021). Sequence quality was assessed using FASTQC, and amplicon sequence variants (ASVs) were identified and classified using NGTax 2.0 with the Silva 138.1 database (Poncheewin et al., 2020). ASVs with a relative abundance of less than 0.1% per sample were discarded to minimize the impact of sequencing and PCR errors. A total of 9,822,362 reads from 136 samples, including controls, were retained for downstream analysis.

Statistical analysis and visualization of microbial community data were performed using R (v.3.6.0) with the vegan (v.2.5-6), phyloseq (v.1.30.0), dplyr (v.0.8.5), ggplot2 (v.3.3.0), and DESeq2 (v.1.26.0) packages. Pearson correlation analyses were conducted to evaluate the relationships between operational parameters, byproduct concentrations, and microbial community abundance. A total of 144 data points were used for the analysis, including all biological replicates. Alpha-diversity metrics (observed ASV richness, Shannon diversity index, and Pielou's evenness) were calculated using the vegan package. Pielou's evenness index was used to visualize the distribution of ASV abundances across samples.

3. Results and discussions

Anaerobic degradation of glucose, glycerol, and casein in open mixed cultures involves a complex cascade of biochemical reactions driven by diverse microbial communities, as illustrated in Fig. 1. These pathways are fundamentally shaped by syntrophic interactions among different microbial groups. In anaerobic mixed culture chain elongation, a key factor influencing pathway direction is the competition between acetogenesis and methanogenesis, with methanogenesis ultimately leading to methane formation (Chen et al., 2016; Shrestha et al., 2023). Notably, even with the addition of 2-bromoethanesulfonate (BES), a known methanogen inhibitor, methanogenic activity and methane production have been observed (Shrestha et al., 2023). Furthermore, pathway direction depends on operational conditions, including electron donor availability, in-situ electron donor production, microbial community composition, pH, hydrogen partial pressure, salinity, and hydraulic retention time (Coma et al., 2016; Han et al., 2018; Joshi et al., 2021; Spirito et al., 2014; Veras et al., 2020; Wang and Yin, 2022). Consequently, the CE pathway can be selectively steered in anaerobic digestion or occur concurrently with methanogenesis, depending on the

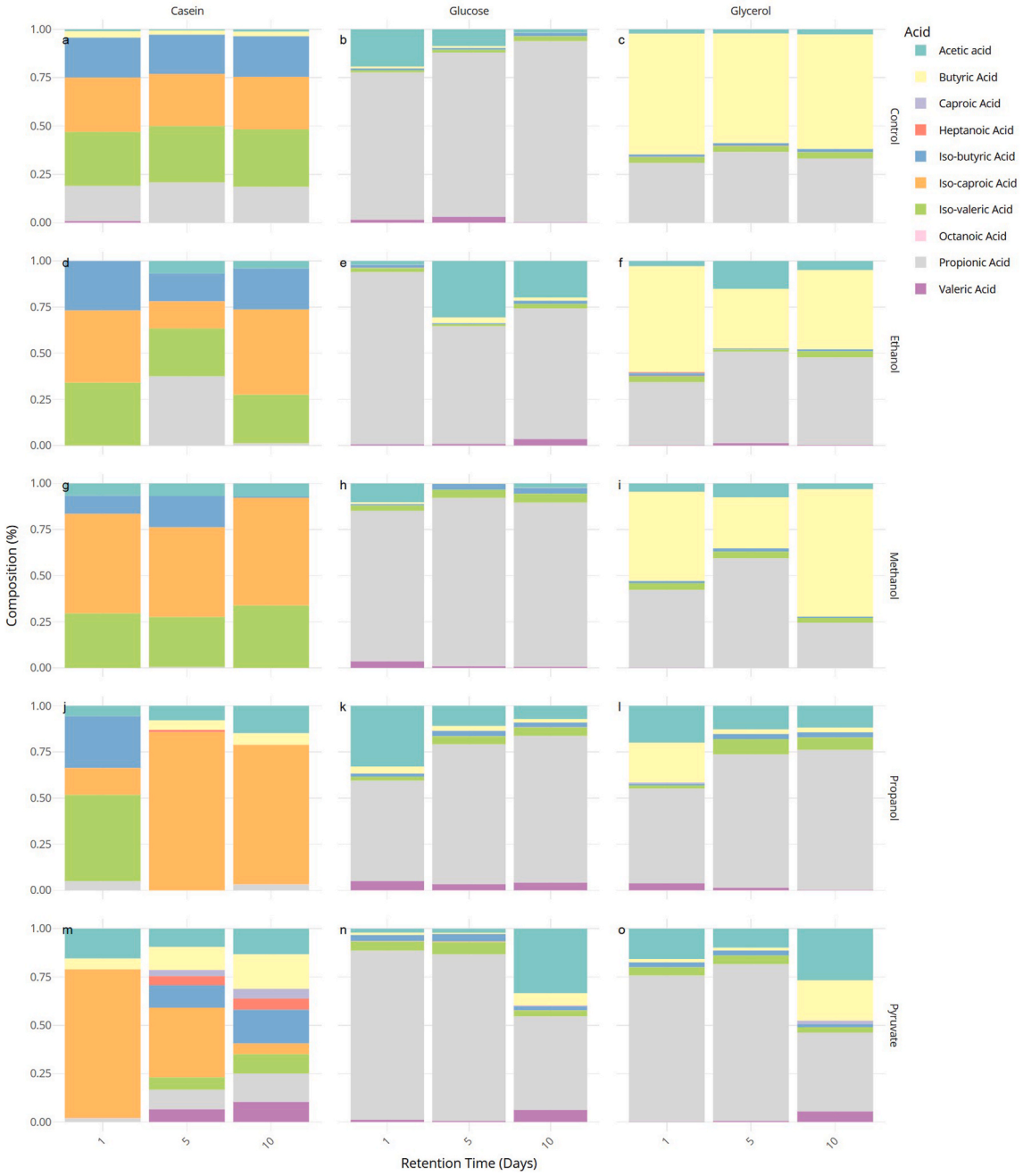

Fig. 3. Carboxylic acid composition at retention times of 1, 5, and 10 days for each carbon source (casein, glucose, glycerol) and electron donor type (control, ethanol, methanol, propanol, pyruvate) highlights the influence of both carbon source and electron donor on microbial metabolism over time, revealing how these factors affect carboxylic acid profiles at each retention time point. This interactive plot displays the mean values of acid concentrations with corresponding standard deviations for each retention time point. It was generated using the Plotly. js library (v2.11.1).

interplay of these factors.

Therefore, in this study, we evaluated the impact of external electron donor addition on the individual degradation of glucose, glycerol, and casein, specifically monitoring the resulting shifts in metabolic pathways toward methanogenesis and chain elongation. The influence of carbon source and electron donor on system performance was assessed through the quantification of metabolite production in both liquid and gaseous phases, coupled with an analysis of the microbial community profile.

3.1. *Effects of carbon source on system performance*

To evaluate the conversion of carbon sources and electron donors into metabolic products, chemical oxygen demand equivalents (mgCOD-eq) were utilized, encompassing total carboxylic acid concentration, carbon source consumption, and alcohol accumulation (Fig. 2.1). Carboxylic acids, including acetic, propionic, butyric, iso-butyric, iso-valeric, valeric, iso-caproic, caproic, heptanoic, and octanoic acids, were quantified to determine carboxylic acid production efficiency. Medium-chain fatty acids (MCFAs), specifically iso-caproic, caproic, heptanoic, and octanoic acids, were used as indicators of chain elongation performance. Previous studies have shown that propionic, butyric, and valeric

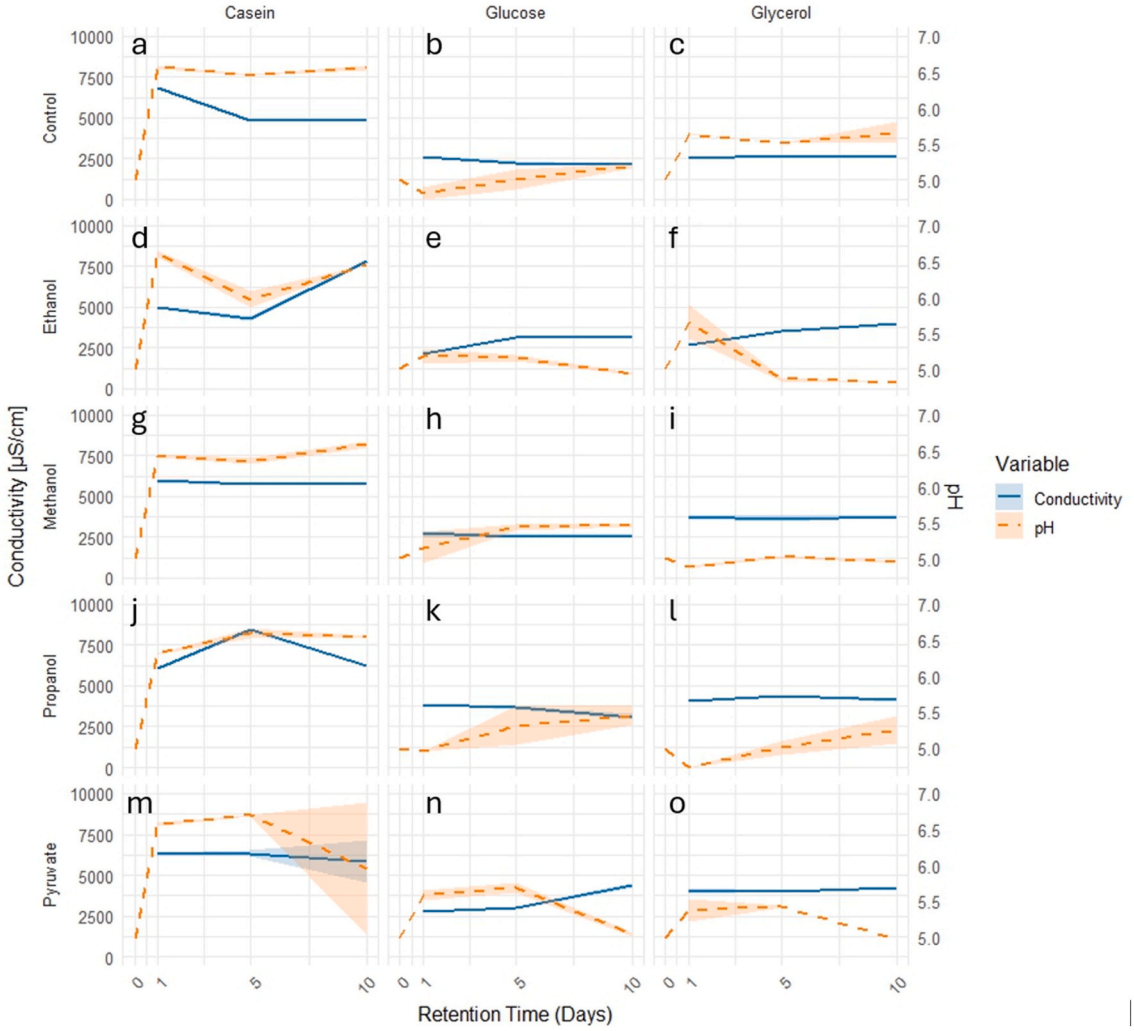

Fig. 4. Temporal profiles of conductivity and pH (secondary axis) at 0, 1, 5, and 10 days of incubation for each carbon source (casein, glucose, glycerol) and electron donor (control, ethanol, methanol, propanol, pyruvate), including standard deviation. Measurements were conducted at 35 °C.

acids, along with their isomers, can be produced from acetate and other single-carbon compounds, such as alcohols, through chain elongation (Chen et al., 2016, 2017; De Smit et al., 2019). Theoretically, chain elongation extends SCFAs by adding two carbon atoms (an acetyl-CoA molecule) per cycle, as illustrated in Fig. 1. In this study, we define chain elongation efficiency as the conversion of SCFAs into MCFAs. The composition of carboxylic acids, expressed as a percentage, is presented in Fig. 3 to highlight variations under different carbon source and electron donor conditions.

Carbon sources significantly impacted both carboxylic acid production and composition. The highest total carboxylic acid concentration (7396 ± 85 mgCODeq/L) was observed on day 10 with the glycerol-methanol combination, achieving a 92% conversion of the initial COD (Fig.2.1i) Butyric acid was the dominant product, accounting for 69% of the total carboxylic acids, followed by propionic acid at 24% (Fig. 3i). Notably, negligible MCFA production was detected in glycerol sets, and the pH was recorded as 4.95 ± 0.3 (Fig. 4). Similarly, Coma et al. (2016) reported that butyrate was the primary byproduct in mixed-culture chain elongation when various carboxylates were supplemented with ethanol, observed on day 10 at pH 5.5 (Coma et al., 2016). Duber et al. (2024) found that lactate-based chain elongation of glycerol by anaerobic mixed cultures primarily yielded butyrate (~40%), with acetate (~20%) as a secondary metabolite (Duber et al., 2024) as well. Similarly, Leng et al. (2019) demonstrated that continuous glycerol fermentation for carboxylate chain elongation predominantly produced acetic and butyric acids, whereas batch operation favoured 1,3-propanediol (1,3-PDO) formation (Leng et al., 2019).

The glycerol and pyruvate combination yielded the second-highest carboxylic acid production, 6431 ± 51 mgCODeq/L on day 10 (Fig.2.1o), with a composition of 40% propionic acid, 27% acetic acid, and 20% butyric acid (Fig. 3o). Only 2.1% of the produced carboxylic acids were MCFAs (exclusively caproic acid), and the pH was measured at 4.93 ± 0.04 (Fig. 4). In some glycerol degradation sets, propionate was the dominant metabolite, with its production enhanced by the type of electron donor. Additionally, sets containing propanol and pyruvate showed dominant propionate production (Fig. 3l and o). Veras et al. (2020) demonstrated that glycerol was primarily converted into propionate in anaerobic mixed culture chain elongation, with the highest Gibbs free energy derived from glycerol-to-propionate conversion. This was followed by propionate elongation into valerate in the presence of ethanol, driven by the thermodynamic favourability of high propionate and ethanol concentrations. Coma et al. (2016) stated that elevated intracellular propionyl-CoA concentrations can drive odd-chain fatty acid synthesis, with propionyl-CoA substituting for acetyl-CoA in the initial fatty acid synthesis step.

This leads to propionate elongation to valerate and subsequently heptanoate. In their experiments using propanol as an electron donor, propionate formation from propanol degradation was the dominant pathway. However, valerate production, resulting from propionate elongation, increased from 11% to 27% of total molar volatile fatty acid

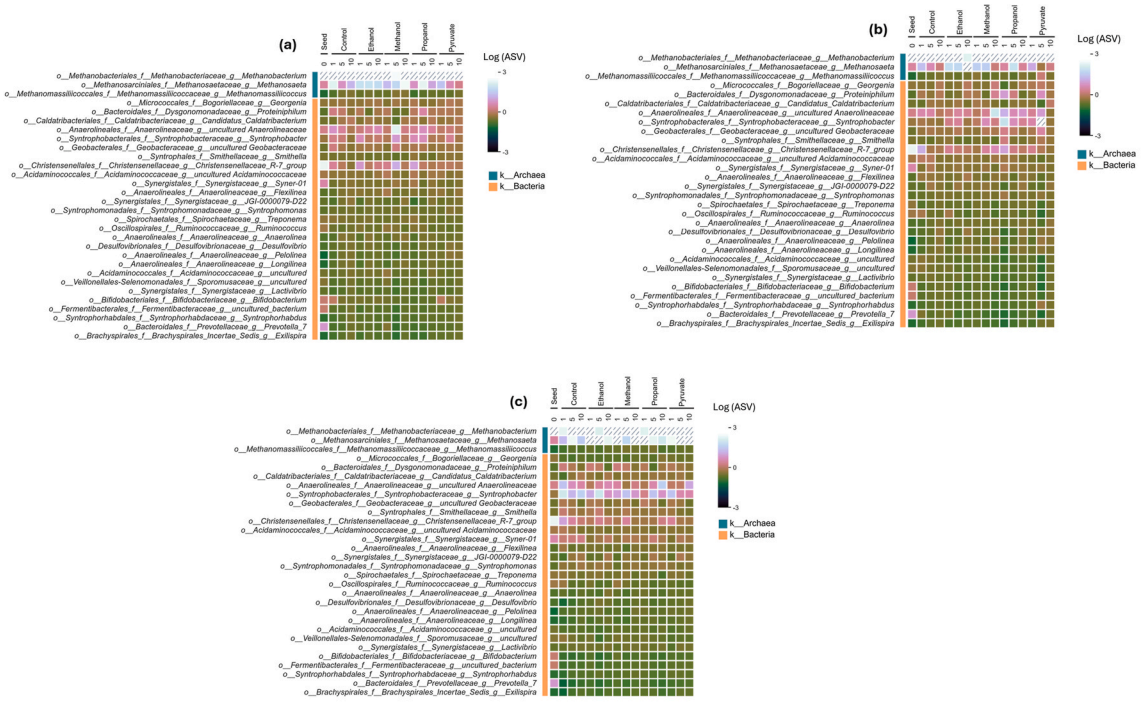

Fig. 5. Heatmap illustrating the distribution of dominant bacterial and archaeal genera across retention times for each electron donor type, under carbon sources of (a) glucose, (b) glycerol, and (c) casein. The colour intensity represents the abundance of each amplicon sequence variant (ASV) normalized with $\log_{10}$ to highlight variations in lower abundance ASVs. The heatmap is based on 16S rRNA amplicon sequence data. The colour scale ranges from white - blue (high ASV abundance on the logarithmic scale) to dark green (low ASV abundance on the logarithmic scale). The grid filled cells indicate the highest abundance.

production (Coma et al., 2016).

These observations align with our findings, where propionate was observed in glycerol degradation, along with iso-valerate production in the propanol set on days 5 and 10. This correspondence suggests that similar elongation routes–initiated from propionate and extended via reverse β-oxidation–were active in our systems, accounting for the accumulation of C5–C6 acids.

Wu et al. (2018) further showed that lactate, when used as the sole carbon source for chain elongation, is primarily converted to propionate due to the existence of a competing acrylate pathway, which shifts the lactate-carbon flux toward propionate production, reducing chain elongation selectivity. This suggests that the type of carbon source and electron donor plays a key role in directing the metabolic pathways toward specific metabolites.

With the glucose-pyruvate combination, a comparable carboxylic acid concentration of 6416 ± 63 mgCODeq/L was achieved by day 10

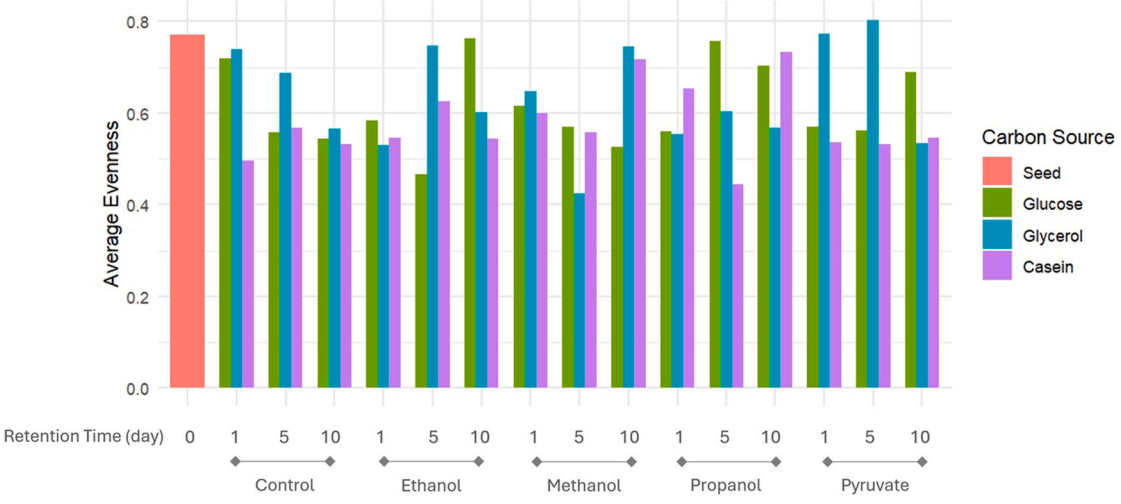

Fig. 6. Evenness index for each set based on carbon source and electron donor across different retention times. The evenness index measures the relative distribution of microbial species in a sample, with values closer to 1.0 indicating a more even distribution and thus more balanced microbial diversity.

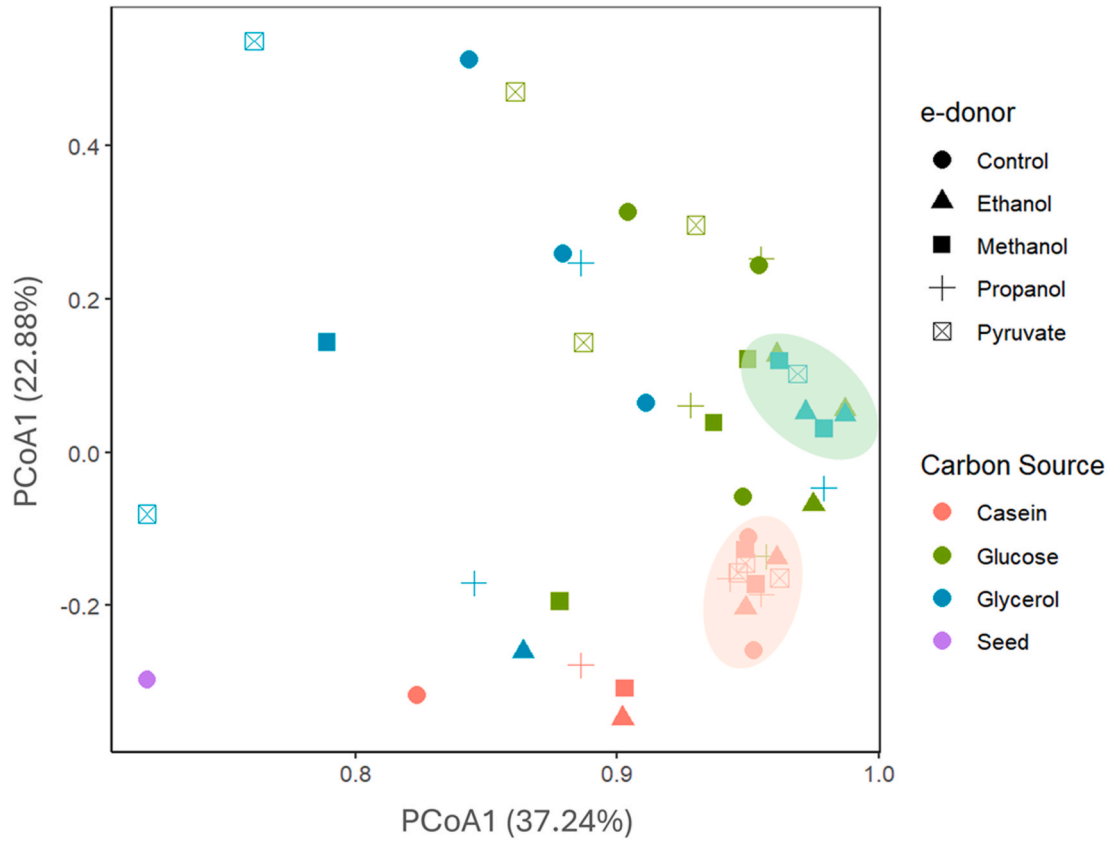

Fig. 7. Principal Coordinates Analysis (PCoA) illustrating the impact of carbon source and electron donor on microbial community structure. Casein carbon source communities cluster tightly, indicating similar community profiles. The seed community is positioned distantly, demonstrating a distinct composition. Ethanol electron donor communities exhibit greater similarity compared to communities utilizing other electron donors.

(Fig 2.1n). The carboxylic acid composition in this set was dominated by propionic acid (48%) and acetic acid (33%), while MCFAs, including iso-caproic, caproic, and heptanoic acids, comprised only 0.65% of the total carboxylic acids (Fig. 3n). The pH was measured at 5.04 ± 0.12 (Fig. 4). ***Propionate was the primary product of glucose degradation, irrespective of the electron donor type*** (Fig. 3), despite its production being less thermodynamically favourable than acetate or butyrate formation (Coma et al., 2016). Consistent with this observation, Chen et al. (2017) reported that 98% of glucose degradation in an anaerobic mixed culture yielded propionate, attributing this to the inhibition of propionate degradation (Chen et al., 2017). In addition to the inhibition of propionate-degrading microorganisms by potential inhibitors, a combination of factors—including the specific microbial community present, environmental conditions, and the metabolic pathways favoured under these conditions—can enhance propionate production while suppressing its degradation, thereby leading to its accumulation in the system.

In contrast to the glucose and glycerol sets, the casein sets exhibited the lowest carboxylic acid and gas production, ranging from 362 to 3305 mgCODeq/L across all retention times. Furthermore, the pH in all casein sets varied between 6.00 and 6.70. Despite the lower carboxylic acid production, casein sets demonstrated the highest MCFA production. Additionally, these sets exhibited the highest conductivity, averaging 6087 ± 1061 μS/cm, compared to 3552 ± 628 μS/cm in glycerol sets and 2948 ± 507 μS/cm in glucose sets (Fig. 4). Correlation analysis (Supplementary Fig. 1) revealed a positive correlation between MCFA production and both pH ($p = 0.741$, $p > 0.01$) and conductivity ($p = 0.702$, $p > 0.01$).

In the anaerobic degradation of casein, protein deamination, leading to total ammoniacal nitrogen (TAN) production, is often the rate-limiting step (Deng et al., 2023). Elevated TAN concentrations can inhibit methanogenesis and promote SCFA accumulation (Deng et al., 2023). The comparatively low carboxylic acid production and high conductivity observed in the casein sets may therefore be attributed to substantial ammonium release resulting from casein hydrolysis.

The control sets of casein degradation supported the findings of Bevilacqua et al. (2022), demonstrating that during anaerobic casein degradation by a mixed microbial culture, external electron donor addition can be bypassed through in-situ electron donor production from the carbon source. While external electron donor addition enhanced the chain elongation pathway in our study, the control sets indicated that this pathway is also viable in its absence.

Within the casein sets, the highest carboxylic acid production (3305 ± 743 mgCODeq/L) was measured in the pyruvate set on day 5 (Fig.2.1m), with a composition primarily consisting of iso-caproic acid (36%), butyric acid (11.8%), iso-butyric acid (11.6%), propionic acid (10.5%), and acetic acid (9.5%) (Fig. 3m). The total MCFA concentration was 1449 ± 210 mgCODeq/L, representing approximately 44% of the total carboxylic acids. The effluent pH in this set was 6.70 (Fig. 4m).

Interestingly, casein-supported fermentations yielded the highest MCFA concentrations despite lower total acid production. This outcome likely results from amino acid-derived electron flow during protein degradation (Deng et al., 2023; Wang et al., 2022). Under anaerobic conditions, amino acids released from casein can participate in

Stickland-type reactions, where paired amino acids act as both electron donors and acceptors, generating reducing equivalents (e.g., NADH or H_2) that can fuel reverse β-oxidation and drive chain elongation (Pavao et al., 2022; Vijande et al., 2024). Moreover, specific amino acids such as leucine, isoleucine, valine, and lysine can be converted to short-chain acyl-CoA intermediates (e.g., butyryl-CoA, isovaleryl-CoA), which serve as precursors for medium-chain carboxylate synthesis (Pavao et al., 2022). Consequently, the combination of amino acid catabolism and internal electron donor generation likely explains the enhanced MCFA formation observed in the casein-fed cultures, despite the relatively low overall carboxylic acid production.

Iso-caproic acid production was observed in the casein set, whereas other carbon sources yielded negligible or minimal amounts of caproic/iso-caproic acid. The highest iso-caproic acid concentrations (472 ± 49.5 and 278 ± 6.2 mgCODeq/, respectively) were obtained in sets supplemented with propanol (5-day retention time) and pyruvate (1-day retention time) as electron donors (Fig. 3j and m). Furthermore, in the casein sets, particularly those supplemented with ethanol, methanol, or propanol, and in the control sets, iso-valeric acid constituted a significant proportion of the total carboxylic acids, ranging from 22% to 56% across different retention times. Similarly, iso-butyric acid production in the casein-containing sets varied from 7% to 35% of the total carboxylic acids across the retention times.

The specific distribution of iso-acids in our results strongly reflects the amino acid composition of the substrate. For instance, the high proportion of iso-valeric acid (22–56%) aligns with the high leucine content of casein, which serves as its direct metabolic precursor (Deng et al., 2023; Stams and Plugge, 2009). Furthermore, our observation of iso-caproic acid suggests that these branched-chain short-chain fatty acids served as primers for the RBO pathway. Unlike glucose-derived elongation which typically begins with acetyl-CoA, iso-caproic acid formation likely involves the addition of acetyl-CoA units to an isovaleryl-CoA primer (De Leeuw et al., 2019; Wu et al., 2024).

From a downstream processing perspective, the prevalence of branched-chain products introduces a trade-off. The close structural similarity between iso- and n-caproic acid can increase the complexity of separation by fractionated distillation or membrane-based processes (Wu et al., 2021; Zhao et al., 2024). However, branched-chain MCFAs typically command a higher market value in specialty applications. Methyl branching confers improved low-temperature fluidity and enhanced oxidative stability, properties that make these compounds attractive precursors for specialty bio-lubricants and high-value fragrance esters (Bart et al., 2013; Máximo et al., 2024). Consequently, the casein-based process shifts the overall value proposition from bulk commodity chemicals toward higher-value specialty intermediates.

From a microbial and ecological perspective, the formation of branched-chain fatty acids has been attributed, at least in part, to bio-isomerization processes. Although bio-isomerization has been reported in several studies, its ecological function remains poorly understood. While isomerization itself does not directly yield growth energy, it has been proposed as a detoxification strategy for inhibitory unbranched short-chain fatty acids, particularly butyrate (Chen et al., 2017). Chen et al. (2017) demonstrated that during anaerobic mixed-culture fermentation of acetate and ethanol, medium-chain fatty acid production was not observed within 40 days, with butyrate accumulating as the dominant metabolite. Subsequently, iso-butyrate formation was detected, suggesting a continuous transformation of butyrate via bio-isomerization. Similarly, Duber et al. (2024) reported iso-butyrate and iso-valerate as dominant by-products of lactate-based chain elongation of glycerol. Although they were also unable to fully elucidate the mechanism of isomerization, their findings support the hypothesis of Chen et al. (2017) that isomerization may serve as a strategy to mitigate the toxic effects of accumulated butyrate/valerate, as unbranched fatty acids are generally more toxic to microbial cells than their corresponding branched forms (Duber et al., 2024). Consequently, understanding and controlling bio-isomerization is essential not only for interpreting microbial community function but also for steering product profiles toward higher-value branched compounds in biobased chemical production systems.

Acidic pH promoted SCFA production, while neutral pH enhanced MCFA production. Another important parameter, the pH of the system, which was significantly altered by the carbon source, plays a critical role in the ionization state of organic acids generated during fermentation. At low pH values (particularly pH < 5.0), a larger fraction of organic acids remains undissociated (Z. Li et al., 2024; Xu et al., 2022). This undissociated form can passively permeate cell membranes, necessitating increased cellular ATP expenditure for active efflux. Consequently, cells may shift away from acetate production, a high ATP-yielding pathway, towards butyrate synthesis, which results in a smaller pH change per mole of glucose and thus reduces energy costs (Z. Li et al., 2024; Wang and Yin, 2022).

This phenomenon of increased undissociated SCFA diffusion at low pH was also observed by Bevilacqua et al. (2022). Consistent with Coma et al. (2016) (Coma et al., 2016), we found that neutral pH conditions enhanced MCFA production, likely due to the inhibitory effects of acidic environments on MCFA synthesis. In our casein sets, the pH shifted towards neutrality (pH 6.5–7) (Fig. 4), a condition not accompanied by methane production (Fig.2.2). Conversely, glucose and glycerol reactors exhibited a more acidic pH (pH < 6). Studies suggest that chain elongation may be constrained by the toxicity of undissociated SCFAs at pH values near the pKa of caproic acid (approximately pH 5.6) (Z. Li et al., 2024; Rahimieh et al., 2024). This observation may explain the increased MCFA production and reduced SCFA production in the neutral casein sets, relative to the acidic glucose and glycerol sets.

3.2. *Effects of electron donor type on system performance*

Electron donors influenced the degradation rate of glycerol. In the control reactors, glycerol degradation proceeded slowly, with 30% remaining after 10 days. In contrast, the addition of methanol, propanol, or pyruvate rapidly accelerated glycerol degradation, achieving near-complete consumption by day 1. Ethanol supplementation also facilitated complete glycerol degradation by day 10, though a substantial portion remained at earlier time points (26% on day 1, 22% on day 5) (Fig 2.2f). Duber et al. (2024) reported 87% glycerol degradation into metabolites within 10 days during lactate-based chain elongation in an anaerobic mixed culture (Duber et al., 2024). Therefore, our results indicate that electron donor addition enhances glycerol degradation in anaerobic digestion. This acceleration can be attributed to improved redox balance and increased availability of reducing equivalents (e.g., NADH, $FADH_2$) that promote glycerol oxidation and subsequent conversion to short-chain intermediates. Electron donors such as methanol, propanol, and pyruvate may also activate specific microbial guilds capable of utilizing glycerol through the reverse β-oxidation pathway, thereby enhancing its overall conversion efficiency.

Due to the readily degradable nature of glucose, the effects of the electron donor type were minimal in these sets. However, in casein sets, electron donor addition, particularly in the control and ethanol sets, significantly impacted casein degradation. In the control, 81% of casein was degraded by day 1, while 13% and 11% remained on days 5 and 10, respectively (Fig.2.1a). These results suggest that the degradation of complex substrates such as proteins is strongly influenced by external redox conditions. The availability of additional electron donors may enhance proteolytic and deaminative processes, indirectly supporting chain elongation by supplying both carbon skeletons and reducing power.

Regarding carboxylic acid production, the influence of electron donor type mirrored its effect on carbon source degradation. In glycerol sets, ethanol, methanol, and pyruvate addition increased carboxylic acid production by 3.16, 3.72, and 3.23-fold, respectively, compared to the control on day 10 (Fig.2.1). Propanol addition also enhanced carboxylic

acid production by 2.3-fold on day 1. In glucose sets, the effects of electron donor addition were less pronounced. In casein sets, pyruvate addition significantly increased carboxylic acid and MCFA production, with 3.03 and 4.92-fold increases on day 5, and 2.22 and 1.34-fold increases on day 10, respectively, compared to the control. These trends indicate that the type of electron donor not only governs substrate degradation but also dictates the metabolic direction of carbon flow. Pyruvate, being a central metabolic intermediate, can directly feed into the acetyl-CoA pool and stimulate reverse β-oxidation, explaining its strong effect on MCFA formation. Similarly, methanol and propanol can provide additional reducing power to drive chain elongation reactions toward longer-chain acids.

The degradation rate of added electron donors was dependent on the electron donor type. Across all carbon source reactors, a substantial portion of ethanol remained on day 1, with 65% in casein reactors, 51% in glycerol reactors, and 27% in glucose reactors. However, ethanol was nearly completely consumed in all reactors by subsequent retention times. Wang and Yin et al. (2022) reported that during ethanol-guided chain elongation, excess ethanol oxidation to acetate can inhibit the conversion of ethanol to MCFAs (Wang and Yin, 2022). This inhibition can be mitigated by adjusting the hydrogen partial pressure of the system, thereby promoting chain elongation from ethanol (Grootscholten et al., 2014). Our results align with these findings, suggesting that transient accumulation of ethanol early in the fermentation may have temporarily shifted the redox balance toward acetate formation before chain elongation became dominant.

In addition to the degradation of the substrate into identified metabolites, some sets exhibited unidentified compounds that accounted for a portion of the missing COD. Even considering that methane production reached up to 200 mg COD/L at maximum (Fig.2.2), a substantial fraction of the COD from the carbon source remains unaccounted for. We hypothesize that this missing COD may have been converted to lactate via the acrylate pathway (Montecchio et al., 2024; Xu et al., 2022), to formate, or to other undetected compounds such as 1, 3-propanediol (Duber et al., 2024).

Likewise, methanol persisted in glucose and glycerol reactors on day 1, with 99% and 89% remaining, respectively, but was negligible at subsequent time points. In contrast, propanol and pyruvate were rapidly degraded in all carbon source reactors by day 1. Coma et al. (2016) demonstrated that methanol does not directly contribute to carboxylate elongation (Coma et al., 2016). Conversely, propanol degradation increased with successive transfers, resulting in an elevated proportion of odd-carbon carboxylates, such as propionate and valerate, in the final product. They concluded that methanol, ethanol, and propanol, but not butanol, are suitable for MCFA production, with ethanol and propanol being the most effective. Acetate-propanol combinations yielded mixtures of both even- and odd-carbon carboxylates, whereas other combinations, including methanol, produced predominantly even-carbon carboxylates (Coma et al., 2016). Together, these observations highlight that external electron donors not only influence substrate degradation kinetics but also shape the metabolic pathways and product spectrum through modulation of redox balance and intermediate pool distribution within the mixed culture.

Longer retention time can enhance MCFA production. Wu et al. (2018) reported that complex substrates, such as those found in liquor-making wastewater, necessitate an extended lag phase, exceeding 8 days, for microbial community acclimation and subsequent degradation. In their study, MCFA production by a mixed microbial culture commenced after 20 days and declined after 27 days. This suggests that adequate lag time is crucial for microbial adaptation to specific substrate degradation. In our study, retention time showed a positive correlation with carboxylic acid production ($r = 0.460$, $p < 0.01$), supporting the importance of retention time in chain elongation performance (Supplementary Fig. 1).

However, several studies have shown that shorter hydraulic retention times can still be sufficient to initiate chain elongation when simpler substrates are used. For instance, Coma et al. (2016), detected elongated products up to C6 from acetate after 9 days, using a mixed microbial culture (Coma et al., 2016). Similarly, Bevilacqua et al. (2022) reported chain elongation of SCFAs to MCFAs within 6 days using anaerobic mixed fermentation, and Smit et al. (2007) demonstrated that 3.95 days were sufficient to observe methanol-based propionate elongation by an anaerobic mixed culture.

In our reactors, the 10-day retention time was adequate to observe chain elongation activity. However, based on these literature findings, the low chain elongation conversion efficiency in the glucose and glycerol reactors could be improved by extending the retention time to 15 or 20 days.

Gas production, including CH_4, CO_2, H_2, and N_2, was observed in glucose and glycerol sets (Fig. 2)***, but not in casein sets***. In both glucose and glycerol sets, gas composition was influenced by electron donor type. Methane (CH_4) production was similar across all electron donors in both glucose and glycerol sets. In the control, CH_4 production was 4.88 $\pm$ 1.2 mmol in glycerol sets and 4.62 $\pm$ 0.8 mmol in glucose sets on day 10. The primary difference between glucose and glycerol sets was hydrogen (H_2) production, which was affected by both carbon source and electron donor type. In the glycerol control, 3.87 $\pm$ 0.5 mmol H_2 was observed, while no H_2 was detected in glucose sets on day 10. Similarly, propanol and pyruvate additions in glycerol sets resulted in 8.3 $\pm$ 0.2 mmol and 10.01 $\pm$ 0.7 mmol H_2, respectively, while no H_2 was produced in glucose sets. Carbon dioxide (CO_2) and nitrogen (N_2) production varied with electron donor type in both glucose and glycerol sets.

3.3. Microbial community profile

Microbial community composition was identified through 16S rRNA amplicon sequencing. Results are presented as the relative abundance of dominant microbial groups at the phylum and family levels. Genus-level data are shown as log10-transformed abundances of individual amplicon sequence variants (ASVs) in Fig. 5.

Microbial community diversity, as represented by the evenness index (Fig. 6), varied across sets. The seed sludge, sourced from anaerobic digester of paper mill wastewater treatment plant, exhibited significantly higher diversity. In glycerol reactors, diversity remained comparable to the seed sludge on days 1 and 5, while it decreased in casein reactors. Coma et al. (2016) suggested that similar class-level microbial groups facilitate chain elongation regardless of the carboxylate substrate. However, our data indicate that substrate selection significantly influenced microbial community composition, as evidenced by the distinct clustering of control reactors compared to the inoculum and successful chain elongation reactors.

Principal Coordinates Analysis (PCoA) (Fig. 7) further revealed distinct microbial community clustering based on substrate and electron donor. Specifically, ethanol-supplemented sets, regardless of glucose or glycerol origin, clustered together, whereas casein sets formed a separate group across most electron donor conditions. Consistent with the diversity analysis, the seed sludge exhibited a significantly different microbial community profile compared to all experimental sets, as demonstrated by the PCoA results.

At the phylum level, the dominant microbial groups were consistent across all experimental sets, although their relative abundances varied according to carbon source and electron donor. The overall microbial community composition revealed the following dominant phyla: *Euryarchaeota* (20.4%), *Chloroflexi* (16.8%), *Firmicutes* (15.7%), *Desulfobacterota* (12.7%), and *Halobacterota* (10.8%). In glucose sets, the phylum distribution was characterized by *Euryarchaeota* (23.5%), *Chloroflexi* (16.5%), and *Firmicutes* (15.9%). Glycerol sets exhibited a similar distribution, with *Euryarchaeota* (22.1%), *Chloroflexi* (18.1%), and *Firmicutes* (15.5%) dominating. In casein sets, the dominant phyla were *Chloroflexi* (15.8%), *Firmicutes* (15.8%), and *Euryarchaeota* (15.5%). The seed sludge (day 0) was primarily composed of *Firmicutes*

(23.8%), *Chloroflexi* (13.7%), *Euryarchaeota* (11.2%), and *Bacteroidota* (9.1%). Despite similar phylum-level profiles, downstream metabolic performance differed substantially among substrate conditions, indicating that functional specialization occurred primarily at lower taxonomic levels.

The microbial community profiles were characterized by a high abundance of methanogens across nearly all sets, irrespective of carbon source and electron donor. While anaerobic chain elongation is typically associated with enrichment of *Firmicutes* phyla (Coma et al., 2016; Han et al., 2018; Joshi et al., 2021), our findings align with observations of significant methanogen presence in similar systems. For instance, Veras et al. (2020) reported a diverse community dominated by *Firmicutes, Proteobacteria, Bacteroidota, and Actinobacteriota* in glycerol-based chain elongation. However, consistent with our results, several studies have noted the persistence of methanogenic activity and high methanogen abundance. Shrestha et al. (2023) observed continued methanogenic activity and dominance of methanogenic archaea despite BES addition. Similarly, De Smit et al. (2019) detected methanogenic activity and abundance even under acidic pH conditions (pH < 5) during methanol-based propionate elongation. Therefore, our microbial community analysis encompassed both bacterial and archaeal groups to comprehensively assess their roles in chain elongation and overall anaerobic degradation.

*Euryarchaeota (*new taxonomic name is *Methanobacteriota)*, which encompasses predominantly hydrogenotrophic methanogens, dominated the microbial community across all sets. Hydrogenotrophic methanogens utilize hydrogen as an electron donor and carbon dioxide as a carbon source to produce methane (Ray et al., 2023; Richards et al., 2016; Shrestha et al., 2023). While *Methanobacteriota* was the most abundant archaeal phylum in glucose (23.5%) and glycerol (22.1%) sets, its relative abundance decreased in casein sets (15.5%). This difference in abundance may contribute to the observed methane production in the glucose and glycerol sets.

The absence of methane in the casein systems, despite detectable methanogen populations, suggests inhibitory conditions linked to protein hydrolysis. Casein degradation leads to elevated TAN levels through amino acid deamination, which can inhibit methanogenic activity by disrupting intracellular pH and coenzyme function (Bonk et al., 2018; Park and Kim, 2016; Sprott and Patel, 1986). Additionally, the metabolic pathways generating iso-acids from branched-chain amino acids consume reducing equivalents and may lower hydrogen availability, thereby suppressing methanogenesis (Stams and Plugge, 2009). These inhibitory effects likely constrained methanogen activity in casein-fed systems, redirecting carbon flow toward acidogenic and elongation pathways.

Furthermore, the higher SCFA production in glucose and glycerol sets suggests a prevalence of hydrogenotrophic methanogenesis over acetoclastic methanogenesis in these sets. Similarly, Shrestha et al. (2023) reported that in ethanol-based chain elongation, *Euryarchaeota*, encompassing predominantly hydrogenotrophic methanogens, constituted over 22% of the active microbial community. Acetoclastic methanogens were absent, likely due to inhibition by the low reactor pH (5.5).

At the family level, the dominant microbial families remained consistent across all sets, although their relative abundances varied depending on the carbon source. Overall, the dominant families across all sets were *Methanobacteriaceae* (28.0%), *Anaerolineaceae* (18.7%), *Methanosaetaceae* (12.5%), *Syntrophobacteraceae* (12.5%), *Christensenellaceae* (6.3%), and *Synergistaceae* (5.4%). In the glucose sets, the family distribution was *Methanobacteriaceae* (28.0%), *Anaerolineaceae* (18.6%), *Methanosaetaceae* (12.2%), *Christensenellaceae* (5.6%), *Syntrophobacteraceae* (4.7%), and *Synergistaceae* (3.6%). In the glycerol sets, the distribution was *Methanobacteriaceae* (26.5%), *Anaerolineaceae* (20.1%), *Methanosaetaceae* (10.2%), *Christensenellaceae* (5.8%), *Syntrophobacteraceae* (5.4%), and *Synergistaceae* (4.9%). In the casein sets, the dominant families were *Methanobacteriaceae* (17.7%), *Anaerolineaceae* (17.5%), *Methanosaetaceae* (15.1%), *Syntrophobacteraceae* (8.4%), *Synergistaceae* (6.9%), and *Christensenellaceae* (4.8%). The seed sludge was primarily composed of *Anaerolineaceae* (14.7%), *Methanobacteriaceae* (12.9%), *Christensenellaceae* (11.5%), and *Synergistaceae* (8.6%).

Consistent with the phylum-level observations, *Methanobacteriaceae*, a family of predominantly hydrogenotrophic methanogens, dominated the microbial community in all sets. The relative abundance of *Methanobacteriaceae* nearly doubled in glucose and glycerol sets compared to the seed sludge. This suggests that acidic pH did not inhibit the growth of hydrogenotrophic methanogens in these systems.

Coma et al. (2016) reported that *Rhodobacteraceae* was the most enriched family in C1 and C3-based chain elongation reactors compared to the seed sludge. However, *Rhodobacteraceae*, a family within the *Pseudomonadota* (synonym *Proteobacteria*) phylum, did not constitute abundant (>5%) groups in our sets. Furthermore, Coma et al. (2016) also detected an unclassified bacterium (Phy7) within the *Clostridia* class in all successful chain elongation reactors, which was also not abundant in our sets. Likewise, diverse microbial groups have been identified in effective carboxylic acid chain elongation systems, suggesting that the relative abundance of specific taxa associated with chain elongation pathways can be significantly influenced by various environmental and operational parameters. Furthermore, the microbial community structure and interspecies interactions also play a crucial role in shaping these microbial populations.

In Fig. 5, the abundance of genus-level members across the experimental sets for each carbon source and electron donor is illustrated. At the genus level, *Methanobacterium* (from the *Methanobacteriaceae* family) was the predominant group across all sets. However, the abundance of *Methanobacterium* varied with carbon source: 30% and 29% in glucose- and glycerol-sets, respectively, and 19% in casein sets.

Song et al. (2024) reported that *Methanobacterium* exhibits syntrophic interactions with *Syntrophomonas*, facilitating long-chain fatty acid (LCFA) degradation. The abundance of these groups is strongly linked to this syntrophic process. LCFA accumulation inhibits methanogenesis by disrupting β-oxidation and inhibiting microbial activity, whereas LCFA alleviation combined with low hydrogen partial pressure stimulates β-oxidation and downstream methanogenesis (Song et al., 2024; Ziels et al., 2017). The presence of *Syntrophomonas* alongside *Methanobacterium* in the glucose and glycerol sets suggests a complex relationship involving interspecies hydrogen transfer. *Syntrophomonas* operates the β-oxidation pathway, converting butyrate and longer-chain fatty acids into acetate and H_2, while *Methanobacterium* consumes the produced H_2 (Meichen et al., 2022; Usman et al., 2022). In this context, *Syntrophomonas* likely facilitated the turnover of fatty acid intermediates via β-oxidation. The H_2 produced during this oxidation was immediately consumed by the hydrogenotrophic *Methanobacterium*. This 'interspecies hydrogen pull' is thermodynamically essential; by keeping the H_2 partial pressure low, the methanogens allowed the β-oxidation of butyrate to remain exergonic, preventing the accumulation of intermediates that could otherwise lead to severe acidification and potential process failure (Hamilton et al., 2015; Junicke et al., 2016).

Methanosaeta (from the *Methanosaetaceae* family) was the second most abundant genus across all sets, with relative abundances of 13.1% in glucose sets, 11.2% in glycerol sets, and 17% in casein sets. While *Methanosaeta*, a known acetoclastic methanogen, primarily converts acetate to methane and carbon dioxide, studies suggest it may possess greater metabolic versatility than previously recognized (Smith and Ingram-Smith, 2007). In contrast to *Methanobacterium*, *Methanosaeta* abundance was higher in the casein sets compared to glucose and glycerol sets. Given that gaseous metabolites, including methane, were below detection limits in the casein sets, the role of *Methanosaeta* in casein degradation remains unclear and requires further investigation, similar to studies elucidating its role in lipid degradation during anaerobic digestion (Kurade et al., 2019).

Regarding bacterial groups, uncultured *Anaerolineaceae* (6.8%) and *Christensenellaceae* group R-7 (5.5%) were dominant in glucose sets. In

glycerol sets, uncultured *Anaerolineaceae* (6.8%) and *Syntrophobacter* (5.9%) were predominant. In casein sets, *Syntrophobacter* (9.5%) and uncultured *Anaerolineaceae* (6.6%) were dominant.

The enrichment of *Syntrophobacter* (9.5%) and *Methanosaeta* (17%) in the casein sets suggests that the community initially adapted to handle the propionate and acetate intermediates derived from amino acid catabolism (Cao et al., 2021; Wu et al., 2023). However, while these taxa were taxonomically dominant, their metabolic function appears to have been decoupled from their abundance. As discussed in Section 3.1, the high TAN levels resulting from casein hydrolysis are known to specifically inhibit the metabolic activity of methanogens without necessarily causing their immediate washout (Bonk et al., 2018; Tian et al., 2018). This creates a metabolic bottleneck: the *Syntrophobacter* requires the methanogens to scavenge H_2 to make propionate oxidation favourable, but the methanogens were functionally suppressed by ammonia (Bonk et al., 2018; Westerholm et al., 2022). This 'stalled' syntropy might explain why these taxa were detected in high relative abundance while methane production remained below detection limits, ultimately redirecting the carbon flux toward the observed accumulation of SCFAs.

The microbial composition of the seed sludge differed significantly from all other experimental sets across all taxonomic levels, as supported by evenness index (Fig. 6) and PCoA results (Fig. 7). The seed sludge (day 0) was primarily composed of *Methanobacterium* (16.8%), *Christensenellaceae* group R-7 (14.2%), *Prevotella_7* (8.2%), and *Syner-01* (6.8%).

The dominant bacterial genera in our study differed substantially from those previously reported in the literature for chain elongation and anaerobic digestion, where *Clostridium* is frequently identified as a key genus (Atasoy et al., 2019; Coma et al., 2016; Duber et al., 2024; Wang and Yin, 2022). For example, Wang and Yin (2022) highlighted *Clostridium, Caproiciproducens, Megasphaera, Eubacterium* as significant genera in carboxylic acid chain elongation (Wang and Yin, 2022). *Clostridium kluyveri*, a well-characterized chain elongator utilizing the reverse β-oxidation (RBO) pathway (Fernández-Blanco et al., 2024), is often considered a model organism for this process.

Overall, our results reveal a distinct genus-level microbial community structure, potentially influenced by variations in pH and electron donor/acceptor availability. Although methanogens dominated most systems, this dominance did not fully suppress chain elongation activity. Moderate methanogenic activity likely stabilized hydrogen partial pressure and redox balance, indirectly supporting reverse β-oxidation and MCFA synthesis (Han et al., 2018; Wang and Yin, 2022; Yang et al., 2024). In contrast, inhibition of methanogenesis in casein-fed systems redirected reducing equivalents toward acidogenesis and elongation, resulting in higher relative MCFA yields despite lower total acid production. This interplay highlights that controlled methanogen activity can coexist with, or even facilitate, efficient MCFA production in mixed-culture systems.

In light of our combined metabolite and microbial community data, and in accordance with Han et al. (2018), further investigations employing systematic multi-omics and metabolic flux analyses are required to elucidate the actual functions and responsible microbial groups in chain elongation and anaerobic digestion pathways. In particular, such approaches could resolve current uncertainties regarding (i) the partitioning of electrons between methanogenesis and chain elongation, (ii) the role of amino acid–derived intermediates and alternative elongation routes, and (iii) the contribution of endogenous electron donors during metabolic transitions. Clarifying these metabolic interactions will be crucial for optimizing electron flow, improving MCFA yield, and enhancing process stability under environmentally relevant conditions.

4. Conclusions

This study investigated the branching dynamics of anaerobic digestion pathways, particularly the competition between methanogenesis and chain elongation, using model substrates representing carbohydrates, lipids, and proteins. By examining both exogenous and endogenous electron donor contributions, we identified that carbon source type and electron donor availability influence degradation kinetics and product selectivity in mixed-culture fermentations. Acidic pH conditions (5.5–6.0) favoured SCFA accumulation, whereas near-neutral conditions (6.7–7.0) promoted MCFA formation, emphasizing the key role of pH in controlling metabolic direction. Casein-fed cultures produced the highest MCFA yields despite lower total acid concentrations, likely due to amino acid-derived electron flow and in situ donor generation. The microbial community composition shifted markedly over 10 days, transitioning from a methanogen-dominated inoculum to chain-elongating consortia, demonstrating the adaptability of anaerobic granular sludge. This insight supports the concept of repurposing anaerobic digesters into chain elongation biorefineries for carbon recovery and value-added product generation. Future research should focus on optimizing pH control, electron flow management, and metabolic flux distribution to enhance MCFA yields and process stability under environmentally relevant conditions. In particular, multi-omics and metabolic flux analyses are required to resolve key uncertainties in electron partitioning between methanogenesis and chain elongation, to characterize amino-acid-derived elongation routes, and to quantify the contribution of endogenous electron donors during metabolic shifts.

CRediT authorship contribution statement

Merve Atasoy: Writing – original draft, Visualization, Supervision, Methodology, Investigation, Formal analysis, Conceptualization. **Nicholas Stucki:** Methodology, Formal analysis, Conceptualization. **Anna Jonkers:** Formal analysis. **David Strik:** Writing – review & editing, Writing – original draft, Conceptualization. **Hauke Smidt:** Supervision, Funding acquisition.

Declaration of competing interest

The authors declare that they have no known competing financial interests or personal relationships that could have appeared to influence the work reported in this paper.

Acknowledgement

The authors would like to thank Christopher Lawson for insightful discussions on potential chain elongation pathways in anaerobic digestion and the role of the fatty acid biosynthesis pathway. The authors acknowledge the Dutch Research Council for its financial contribution to the UNLOCK Project (NWO:184.035.007 and NRGWI. obrug. 2018.005).

Appendix A. Supplementary data

Supplementary data to this article can be found online at https://doi.org/10.1016/j.jenvman.2026.128829.

Data availability

Data will be made available on request.

References

Agler, M.T., Wrenn, B.A., Zinder, S.H., Angenent, L.T., 2011. Waste to bioproduct conversion with undefined mixed cultures: the carboxylate platform. Trends Biotechnol. https://doi.org/10.1016/j.tibtech.2010.11.006.

Angenent, L.T., Richter, H., Buckel, W., Spirito, C.M., Steinbusch, K.J.J., Plugge, C.M., Strik, D.P.B.T.B., Grootscholten, T.I.M., Buisman, C.J.N., Hamelers, H.V.M., 2016. Chain elongation with reactor microbiomes: open-culture biotechnology to produce biochemicals. Environ. Sci. Technol. https://doi.org/10.1021/acs.est.5b04847.

Atasoy, M., Eyice, O., Schnürer, A., Cetecioglu, Z., 2019. Volatile fatty acids production via mixed culture fermentation: revealing the link between pH, inoculum type and

bacterial composition. Bioresour. Technol. 292. https://doi.org/10.1016/j.biortech.2019.121889.
Atasoy, M., Owusu-Agyeman, I., Plaza, E., Cetecioglu, Z., 2018. Bio-based volatile fatty acid production and recovery from waste streams: current status and future challenges. Bioresour. Technol. https://doi.org/10.1016/j.biortech.2018.07.042.
Bart, J.C.J., Gucciardi, E., Cavallaro, S., 2013. 6 - chemical transformations of renewable lubricant feedstocks. In: Bart, J.C.J., Gucciardi, E., Cavallaro, S. (Eds.), Biolubricants. Woodhead Publishing, pp. 249–350. https://doi.org/10.1533/9780857096326.249.
Bevilacqua, R., Regueira, A., Mauricio-Iglesias, M., Lema, J.M., Carballa, M., 2022. Chain elongation may occur in protein mixed-culture fermentation without supplementing electron donor compounds. J. Environ. Chem. Eng. 10. https://doi.org/10.1016/j.jece.2021.106943.
Bonk, F., Popp, D., Weinrich, S., Sträuber, H., Kleinsteuber, S., Harms, H., Centler, F., 2018. Ammonia inhibition of anaerobic volatile fatty acid degrading microbial communities. Front. Microbiol. 9. https://doi.org/10.3389/fmicb.2018.02921.
Candry, P., Radić, L., Favere, J., Carvajal-Arroyo, J.M., Rabaey, K., Ganigué, R., 2020. Mildly acidic pH selects for chain elongation to caproic acid over alternative pathways during lactic acid fermentation. Water Res. 186. https://doi.org/10.1016/j.watres.2020.116396.
Cao, L., Cox, C.D., He, Q., 2021. Patterns of syntrophic interactions in methanogenic conversion of propionate. Appl. Microbiol. Biotechnol. 105, 8937–8949. https://doi.org/10.1007/s00253-021-11645-9.
Caporaso, J.G., Lauber, C.L., Walters, W.A., Berg-Lyons, D., Lozupone, C.A., Turnbaugh, P.J., Fierer, N., Knight, R., 2011. Global patterns of 16S rRNA diversity at a depth of millions of sequences per sample. Proc. Natl. Acad. Sci. U. S. A. 108, 4516–4522. https://doi.org/10.1073/pnas.1000080107.
Chatzipanagiotou, K.R., Soekhoe, V., Jourdin, L., Buisman, C.J.N., Bitter, J.H., Strik, D.P.B.T.B., 2021. Catalytic cooperation between a copper oxide electrocatalyst and a microbial community for microbial electrosynthesis. ChemPlusChem 86, 763–777. https://doi.org/10.1002/cplu.202100119.
Chen, W.S., Huang, S., Strik, D.P.B.T.B., Buisman, C.J.N., 2017. Isobutyrate biosynthesis via methanol chain elongation: converting organic wastes to platform chemicals. J. Chem. Technol. Biotechnol. 92, 1370–1379. https://doi.org/10.1002/jctb.5132.
Chen, W.S., Ye, Y., Steinbusch, K.J.J., Strik, D.P.B.T.B., Buisman, C.J.N., 2016. Methanol as an alternative electron donor in chain elongation for butyrate and caproate formation. Biomass Bioenergy 93, 201–208. https://doi.org/10.1016/j.biombioe.2016.07.008.
Coma, M., Vilchez-Vargas, R., Roume, H., Jauregui, R., Pieper, D.H., Rabaey, K., 2016. Product diversity linked to substrate usage in chain elongation by mixed-culture fermentation. Environ. Sci. Technol. 50, 6467–6476. https://doi.org/10.1021/acs.est.5b06021.
Dahiya, S., Lingam, Y., Venkata Mohan, S., 2023. Understanding acidogenesis towards green hydrogen and volatile fatty acid production – critical analysis and circular economy perspective. Chem. Eng. J. https://doi.org/10.1016/j.cej.2023.141550.
De Leeuw, K.D., Buisman, C.J.N., Strik, D.P.B.T.B., 2019. Branched medium chain fatty acids: Iso-caproate formation from iso-butyrate broadens the product spectrum for microbial chain elongation. Environ. Sci. Technol. 53, 7704–7713. https://doi.org/10.1021/acs.est.8b07256.
De Smit, S.M., De Leeuw, K.D., Buisman, C.J.N., Strik, D.P.B.T.B., 2019. Continuous n-valerate formation from propionate and methanol in an anaerobic chain elongation open-culture bioreactor. Biotechnol. Biofuels 12. https://doi.org/10.1186/s13068-019-1468-x.
Deng, Z., Ferreira, A.L.M., Spanjers, H., van Lier, J.B., 2023. Anaerobic protein degradation: effects of protein structural complexity, protein concentrations, carbohydrates, and volatile fatty acids. Bioresour. Technol. Rep. 22. https://doi.org/10.1016/j.biteb.2023.101501.
Duber, A., Zagrodnik, R., Juzwa, W., Gutowska, N., Oleskowicz-Popiel, P., 2024. Simultaneous medium chain carboxylic acids and 1,3-propanediol production in a bioaugmented lactate-based chain elongation induced with glycerol. Bioresour. Technol. 393. https://doi.org/10.1016/j.biortech.2023.130123.
Fernández-Blanco, C., Veiga, M.C., Kennes, C., 2024. Carbon dioxide as key player in chain elongation and growth of clostridium kluyveri: insights from batch and bioreactor studies. Bioresour. Technol. 394. https://doi.org/10.1016/j.biortech.2023.130192.
Fernández-Blanco, C., Veiga, M.C., Kennes, C., 2023. Effect of pH and medium composition on chain elongation with Megasphaera hexanoica producing C4-C8 fatty acids. Front. Microbiol. 14. https://doi.org/10.3389/fmicb.2023.1281103.
Grootscholten, T.I.M., Strik, D.P.B.T.B., Steinbusch, K.J.J., Buisman, C.J.N., Hamelers, H.V.M., 2014. Two-stage medium chain fatty acid (MCFA) production from municipal solid waste and ethanol. Appl. Energy 116, 223–229. https://doi.org/10.1016/j.apenergy.2013.11.061.
Guo, H., Ji, M., Du, T., Xu, W., Liu, J., Bai, R., Teng, Z., Li, T., 2023. Salt stress altered anaerobic microbial community and carbon metabolism characteristics: the trade-off between methanogenesis and chain elongation. J. Environ. Manag. 341. https://doi.org/10.1016/j.jenvman.2023.118111.
Hamilton, J.J., Calixto Contreras, M., Reed, J.L., 2015. Thermodynamics and H2 transfer in a methanogenic, syntrophic community. PLoS Comput. Biol. 11. https://doi.org/10.1371/journal.pcbi.1004364.
Han, W., He, P., Shao, L., Lü, F., 2018. Metabolic interactions of a chain elongation microbiome. Appl. Environ. Microbiol. 84. https://doi.org/10.1128/AEM.01614-18.
Hoelzle, R.D., Virdis, B., Batstone, D.J., 2014. Regulation mechanisms in mixed and pure culture microbial fermentation. Biotechnol. Bioeng. 111, 2139–2154. https://doi.org/10.1002/bit.25321/abstract.
Holtzapple, M.T., Wu, H., Weimer, P.J., Dalke, R., Granda, C.B., Mai, J., Urgun-Demirtas, M., 2022. Microbial communities for valorizing biomass using the carboxylate platform to produce volatile fatty acids: a review. Bioresour. Technol. https://doi.org/10.1016/j.biortech.2021.126253.
Jin, Y., de Leeuw, K.D., Strik, D.P.B.T.B., 2025. Co-fermentation of crotonate and chain elongation substrates towards mixed bioplastic/organic waste recovery. Chem. Eng. J. 517. https://doi.org/10.1016/j.cej.2025.164552.
Joshi, S., Robles, A., Aguiar, S., Delgado, A.G., 2021. The occurrence and ecology of microbial chain elongation of carboxylates in soils. ISME J. 15, 1907–1918. https://doi.org/10.1038/s41396-021-00893-2.
Junicke, H., van Loosdrecht, M.C.M., Kleerebezem, R., 2016. Kinetic and thermodynamic control of butyrate conversion in non-defined methanogenic communities. Appl. Microbiol. Biotechnol. 100, 915–925. https://doi.org/10.1007/s00253-015-6971-9.
Klindworth, A., Pruesse, E., Schweer, T., Peplies, J., Quast, C., Horn, M., Glöckner, F.O., 2013. Evaluation of general 16S ribosomal RNA gene PCR primers for classical and next-generation sequencing-based diversity studies. Nucleic Acids Res. 41. https://doi.org/10.1093/nar/gks808.
Koehorst, J., Nijsse, B., 2021. Quality assessment, amplicon classification and functional prediction [WWW Document]. https://workflowhub.eu/workflows/154?version=2.
Kurade, M.B., Saha, S., Salama, E.S., Patil, S.M., Govindwar, S.P., Jeon, B.H., 2019. Acetoclastic methanogenesis led by methanosarcina in anaerobic co-digestion of fats, oil and grease for enhanced production of methane. Bioresour. Technol. 272, 351–359. https://doi.org/10.1016/j.biortech.2018.10.047.
Leng, L., Nobu, M.K., Narihiro, T., Yang, P., Amy Tan, G.Y., Lee, P.H., 2019. Shaping microbial consortia in coupling glycerol fermentation and carboxylate chain elongation for Co-production of 1,3-propanediol and caproate: pathways and mechanisms. Water Res. 148, 281–291. https://doi.org/10.1016/j.watres.2018.10.063.
Li, X., Lei, X., Guo, Z., Yan, Z., Gu, X., Xu, X., Al-Hazmi, H.E., Xue, G., Xu, J., Oleskowicz-Popiel, P., Makinia, J., 2024. Enhancing chain-elongating microbiomes: sequential fungi-bacteria cooperation for efficient food waste upgrading using endogenous electron donors. Chem. Eng. J. 488. https://doi.org/10.1016/j.cej.2024.150849.
Li, Z., Qiu, S., Xu, J., Ge, S., 2024. Effect of undissociated n-Caproic acid on methanogen activity and subsequent recovery: methane anabolism and community structure. ACS ES&T Eng. 4, 706–716. https://doi.org/10.1021/acsestengg.3c00393.
Marzban, N., Psarianos, M., Herrmann, C., Schulz-Nielsen, L., Olszewska-Widdrat, A., Arefi, A., Pecenka, R., Grundmann, P., Schlüter, O.K., Hoffmann, T., Rotter, V.S., Nikoloski, Z., Sturm, B., 2025. Smart integrated biorefineries in bioeconomy: a concept toward zero-waste, emission reduction, and self-sufficient energy production. Biofuel Research Journal 12, 2319–2349. https://doi.org/10.18331/BRJ2025.12.1.4.
Máximo, F., Bastida, J., Montiel, C., Gómez, M., Murcia, M.D., Barqueros, C., Ortega-Requena, S., 2024. Branched saturated esters and diesters: sustainable synthesis of excellent biolubricants. Catal. Today 429, 114509. https://doi.org/10.1016/j.cattod.2024.114509.
Meichen, S., Zhijian, S., Chao, Z., Yalei, Z., Shicheng, Z., Gang, L., 2022. Novel long-chain fatty acid (LCFA)-degrading bacteria and pathways in anaerobic digestion promoted by hydrochar as revealed by genome-centric metatranscriptomics analysis. Appl. Environ. Microbiol. 88. https://doi.org/10.1128/aem.01042-22.
Montecchio, D., Gazzola, G., Gallipoli, A., Gianico, A., Braguglia, C.M., 2024. Medium chain fatty acids production from Food Waste via homolactic fermentation and lactate/ethanol elongation: Electron balance and thermodynamic assessment. Waste Manag. 177, 289–297. https://doi.org/10.1016/j.wasman.2024.01.049.
OECD, 2006. OECD GUIDELINES FOR THE TESTING OF CHEMICALS Anaerobic Biodegradability of Organic Compounds in Digested Sludge: by Measurement of Gas Production INTRODUCTION.
Park, S., Kim, M., 2016. Effect of ammonia on anaerobic degradation of amino acids. KSCE J. Civ. Eng. 20, 129–136. https://doi.org/10.1007/s12205-015-0240-4.
Pavao, A., Graham, M., Arrieta-Ortiz, M.L., Immanuel, S.R.C., Baliga, N.S., Bry, L., 2022. Reconsidering the in vivo functions of Clostridial Stickland amino acid fermentations. Anaerobe. https://doi.org/10.1016/j.anaerobe.2022.102600.
Rahimieh, A., Akhavan, G., Mousazadehgavan, M., Mehriar, M., Javadi, A., 2024. Propionate production and degradation in the biological wastewater treatment: a mini review on the role of additives in anaerobic digestion. Desalination Water Treat. https://doi.org/10.1016/j.dwt.2024.100555.
Ray, S., Kuppam, C., Pandit, S., Kumar, P., 2023. Biogas upgrading by hydrogenotrophic methanogens: an overview. Waste Biomass Valoriz. 14, 537–552. https://doi.org/10.1007/s12649-022-01888-6.
Reyhanitash, E., Zaalberg, B., Kersten, S.R.A., Schuur, B., 2016. Extraction of volatile fatty acids from fermented wastewater. Sep. Purif. Technol. 161, 61–68. https://doi.org/10.1016/j.seppur.2016.01.037.
Richards, M.A., Lie, T.J., Zhang, J., Ragsdale, S.W., Leigh, J.A., Price, N.D., 2016. Exploring hydrogenotrophic methanogenesis: a genome scale metabolic reconstruction of Methanococcus maripaludis. J. Bacteriol. 198, 3379–3390. https://doi.org/10.1128/JB.00571-16.
Scarborough, M.J., Lawson, C.E., Hamilton, J.J., Donohue, T.J., Noguera, D.R., 2018. Metatranscriptomic and Thermodynamic Insights into Medium-Chain Fatty Acid Production Using an Anaerobic Microbiome.
Shrestha, S., Colcord, B., Fonoll, X., Raskin, L., 2022. Fate of influent microbial populations during medium chain carboxylic acid recovery from brewery and pre-fermented food waste streams. Environ. Sci. 8, 257–269. https://doi.org/10.1039/d1ew00656h.
Shrestha, S., Xue, S., Raskin, L., 2023. Competitive reactions during ethanol chain elongation were temporarily suppressed by increasing hydrogen partial pressure through methanogenesis inhibition. Environ. Sci. Technol. 57, 3369–3379. https://doi.org/10.1021/acs.est.2c09014.
Sikora, A., Detman, A., Mielecki, D., Chojnacka, A., Błaszczyk, M., 2018. Searching for metabolic pathways of anaerobic digestion: a useful list of the key enzymes. In:

Banu, J.R. (Ed.), Anaerobic Digestion. IntechOpen, Rijeka. https://doi.org/10.5772/intechopen.81256.
Singh, A., Schnürer, A., Dolfing, J., Westerholm, M., 2023. Syntrophic entanglements for propionate and acetate oxidation under thermophilic and high-ammonia conditions. ISME J. 17, 1966–1978. https://doi.org/10.1038/s41396-023-01504-y.
Smith, K.S., Ingram-Smith, C., 2007. Methanosaeta, the forgotten methanogen? Trends Microbiol. 15, 150–155. https://doi.org/10.1016/j.tim.2007.02.002.
Song, L., Ye, M., Wang, C., Ren, Y., Li, D., Ha, J., Qin, Y., Li, Q., Niu, Q., Li, Y.Y., 2024. Methanogenic degradation of long-chain fatty acids associated with syntrophic microbial dynamics during thermophilic AnMBR treatment of lipid-rich dairy wastes. Chem. Eng. J. 498. https://doi.org/10.1016/j.cej.2024.155702.
Spirito, C.M., Richter, H., Rabaey, K., Stams, A.J.M., Angenent, L.T., 2014. Chain elongation in anaerobic reactor microbiomes to recover resources from waste. Curr. Opin. Biotechnol. https://doi.org/10.1016/j.copbio.2014.01.003.
Sprott, G.D., Patel, G.B., 1986. Ammonia toxicity in pure cultures of methanogenic bacteria. Syst. Appl. Microbiol. 7, 358–363. https://doi.org/10.1016/S0723-2020(86)80034-0.
Stamatopoulou, P., Malkowski, J., Conrado, L., Brown, K., Scarborough, M., 2020. Fermentation of organic residues to beneficial chemicals: a review of medium-chain fatty acid production. Processes. https://doi.org/10.3390/pr8121571.
Stams, A.J.M., Plugge, C.M., 2009. Electron transfer in syntrophic communities of anaerobic bacteria and archaea. Nat. Rev. Microbiol. https://doi.org/10.1038/nrmicro2166.
Tian, H., Fotidis, I.A., Kissas, K., Angelidaki, I., 2018. Effect of different ammonia sources on aceticlastic and hydrogenotrophic methanogens. Bioresour. Technol. 250, 390–397. https://doi.org/10.1016/j.biortech.2017.11.081.
Undiandeye, J., Gallegos, D., Bonatelli, M.L., Kleinsteuber, S., Bin-Hudari, M.S., Abdulkadir, N., Stinner, W., Sträuber, H., 2024. Medium-chain carboxylates production from plant waste: kinetic study and effect of an enriched microbiome. Biotechnology for Biofuels and Bioproducts 17. https://doi.org/10.1186/s13068-024-02528-y.
Usman, M., Zhao, S., Jeon, B.-H., Salama, E.-S., Li, X., 2022. Microbial β-oxidation of synthetic long-chain fatty acids to improve lipid biomethanation. Water Res. 213, 118164. https://doi.org/10.1016/j.watres.2022.118164.
Veras, S.T.S., Cavalcante, W.A., Gehring, T.A., Ribeiro, A.R., Ferreira, T.J.T., Kato, M.T., Rojas-Ojeda, P., Sanz-Martin, J.L., Leitão, R.C., 2020. Anaerobic production of valeric acid from crude glycerol via chain elongation. Int. J. Environ. Sci. Technol. 17, 1847–1858. https://doi.org/10.1007/s13762-019-02562-6.
Vijande, C., Bevilacqua, R., Balboa, S., Carballa, M., 2024. Altering operational conditions during protein fermentation to volatile fatty acids modifies the associated bacterial community. Microb. Biotechnol. 17. https://doi.org/10.1111/1751-7915.14505.
Wang, J., Yin, Y., 2022. Biological production of medium-chain carboxylates through chain elongation: an overview. Biotechnol. Adv. https://doi.org/10.1016/j.biotechadv.2021.107882.
Wang, S., Ping, Q., Li, Y., 2022. Comprehensively understanding metabolic pathways of protein during the anaerobic digestion of waste activated sludge. Chemosphere 297. https://doi.org/10.1016/j.chemosphere.2022.134117.
Westerholm, M., Calusinska, M., Dolfing, J., 2022. Syntrophic propionate-oxidizing bacteria in methanogenic systems. FEMS Microbiol. Rev. https://doi.org/10.1093/femsre/fuab057.
Wu, L., Wei, W., Chen, Z., Shi, X., Qian, J., Ni, B.J., 2024. Novel anaerobic fermentation paradigm of producing medium-chain fatty acids from food wastes with self-produced ethanol as electron donor. Chem. Eng. J. 483. https://doi.org/10.1016/j.cej.2024.149236.
Wu, P., Ding, P., Cao, Q. hao, Zhang, C., Fu, B., Liu, Hong bo, Chen, C., jun, Liu, He, 2023. Amino acids as in-situ electron donors drive medium chain fatty acids production from sludge acidogenic fermentation liquid by electro-fermentation enhancement. Chem. Eng. J. 476. https://doi.org/10.1016/j.cej.2023.146537.
Wu, Q., Guo, W., Bao, X., Meng, X., Yin, R., Du, J., Zheng, H., Feng, X., Luo, H., Ren, N., 2018. Upgrading liquor-making wastewater into medium chain fatty acid: insights into co-electron donors, key microflora, and energy harvest. Water Res. 145, 650–659. https://doi.org/10.1016/j.watres.2018.08.046.
Wu, Q., Jiang, Y., Chen, Y., Liu, M., Bao, X., Guo, W., 2021. Opportunities and challenges in microbial medium chain fatty acids production from waste biomass. Bioresour. Technol. 340, 125633. https://doi.org/10.1016/j.biortech.2021.125633.
Xu, X., Gu, X., Ye, T., Liu, Yanbiao, Liu, Yanan, Xue, G., Li, X., Makinia, J., 2022. Overcoming carboxylic acid inhibition by granular consortia in high-load liquefied food waste fermentation for efficient lactate accumulation. J. Clean. Prod. 369, 133438. https://doi.org/10.1016/j.jclepro.2022.133438.
Yang, P., Li, X., Zhuang, H., Liu, M., He, S., 2024. Metabolic interactions in chain elongation system with granular activated carbon for medium-chain carboxylates production. J. Environ. Chem. Eng. 12. https://doi.org/10.1016/j.jece.2024.112070.
Zacharof, M.P., Lovitt, R.W., 2014. Recovery of volatile fatty acids (VFA) from complex waste effluents using membranes. Water Sci. Technol. 69, 495–503. https://doi.org/10.2166/wst.2013.717.
Zhao, J., Ma, H., Gao, M., Qian, D., Wang, Q., Shiung Lam, S., 2024. Advancements in medium chain fatty acids production through chain elongation: key mechanisms and innovative solutions for overcoming rate-limiting steps. Bioresour. Technol. 408, 131133. https://doi.org/10.1016/j.biortech.2024.131133.
Ziels, R.M., Beck, D.A.C., Stensel, H.D., 2017. Long-chain fatty acid feeding frequency in anaerobic codigestion impacts syntrophic community structure and biokinetics. Water Res. 117, 218–229. https://doi.org/10.1016/j.watres.2017.03.060.